

## Articles

## Unusual Strong Ortho Effects in the Rearrangement of Binuclear Gold(I) Complexes

Holger L. Hermann,<sup>†</sup> Peter Schwerdtfeger,<sup>\*,†</sup> Fabian Mohr,<sup>‡,§</sup> and Suresh K. Bhargava<sup>\*,‡</sup>

Department of Chemistry, The University of Auckland, Private Bag 92019, Auckland, New Zealand, and Department of Applied Chemistry, RMIT University, GPO Box 2476V, Melbourne, Victoria 3001, Australia

Received December 19, 2002

Ab-initio calculations using the binuclear model compounds  $[\text{Au}_2\text{X}_2(\mu\text{-L})_2]$  ( $\text{L} = \text{C}_6\text{H}_4\text{PH}_2$ , 5-MeC<sub>6</sub>H<sub>4</sub>PH<sub>2</sub>, and 6-MeC<sub>6</sub>H<sub>4</sub>PH<sub>2</sub> and  $\text{X} = \text{Cl}$ ,  $\text{Br}$ , and  $\text{I}$ ) show that the 6-methyl substituent energetically favors isomerization to a gold(I)/gold(III) species and also sterically blocks the C–C coupling reaction of this complex. These findings are in excellent agreement with experimental data for this system. Furthermore, these results demonstrate that partial opening of the Au(III)–P bond is the key step in the sequence leading to C–C coupling.

## 1. Introduction

A wide variety of binuclear compounds containing gold(I) atoms held in close proximity by a pair of bifunctional ligands is known. Examples of such ligands include dithiocarbamate,<sup>1–3</sup> bis(diphenylphosphino)methane,<sup>4–6</sup> (2-pyridyl)dimethylphosphine,<sup>7</sup> methyl-enethiophosphinate,<sup>8</sup> and phosphorus bis(yliides).<sup>9,10</sup> The digold(I) complexes characteristically undergo oxidative additions with halogens, pseudohalogens, and, in the case of the bis(yliides), alkyl halides to give either metal–metal bonded digold(II) compounds or hetero-valent gold(I)/gold(III) compounds; sometimes both can be isolated depending on the conditions.<sup>8–17</sup> Reaction

with an additional equivalent of halogen can give binuclear digold(III) compounds.<sup>11,18,19</sup>

Binuclear cycloaurated complexes  $[\text{Au}_2(\mu\text{-C}_6\text{H}_4\text{PR}_2)_2]$  ( $\text{R} = \text{Ph}$ ,  $\text{Et}$ ) undergo oxidative addition of halogens or dibenzoyl peroxide to give symmetrical digold(II) compounds  $[\text{Au}_2\text{X}_2(\mu\text{-C}_6\text{H}_4\text{PR}_2)_2]$  ( $\text{R} = \text{Ph}$ ,  $\text{Et}$ ;  $\text{X} = \text{Cl}$ ,  $\text{Br}$ ,  $\text{I}$ ,  $\text{O}_2\text{CPh}$ ).<sup>20–22</sup> Uniquely, in the cases of  $\text{X} = \text{Cl}$ ,  $\text{Br}$ , or  $\text{I}$ , the compounds rearrange spontaneously by coupling of the  $\text{C}_6\text{H}_4\text{PPh}_2$  units to give digold(I) complexes of 2,2'-(biphenyl)bis(diphenylphosphine),  $[\text{Au}_2\text{X}_2(2,2'\text{-Ph}_2\text{-PC}_6\text{H}_4\text{C}_6\text{H}_4\text{PR}_2)]$  ( $\text{R} = \text{Ph}$ ,  $\text{Et}$ ) (Scheme 1).<sup>21,22</sup>

More recent work has shown that when the bridging ligand contains methyl substituents in the 5-positions (i.e., para to phosphorus), similar reactivity is observed (Scheme 1).<sup>23</sup> Although the C–C coupling reactions are first-order with respect to digold(II) complex, it has been suggested that these are multistep processes. Scheme

\* Corresponding authors. E-mail: schwerdt@ccu1.auckland.ac.nz; suresh.bhargava@rmit.edu.au.

<sup>†</sup> The University of Auckland.

<sup>‡</sup> RMIT University.

<sup>§</sup> Present address: Department of Chemistry, The University of Western Ontario, London, N6A 5B7, Ontario, Canada.

(1) Åkerström, S. *Ark. Kemi* **1959**, *14*, 387–401.

(2) Hesse, R.; Jennische, P. *Acta Chem. Scand.* **1972**, *26*, 3855–3864.

(3) Heinrich, D. D.; Wang, J. C.; Fackler, J. P., Jr. *Acta Crystallogr., Sect. C: Cryst. Struct. Commun.* **1990**, *46*, 1444–1447.

(4) Schmidbaur, H.; Wohlleben, A.; Schubert, U.; Frank, A.; Huttner, G. *Chem. Ber.* **1977**, *110*, 2751–2757.

(5) Porter, C. C.; Khan, M. N. I.; King, C.; Fackler, J. P., Jr. *Acta Crystallogr., Sect. C: Cryst. Struct. Commun.* **1989**, *45*, 947–949.

(6) Khan, M. N. I.; King, C.; Heinrich, D. D.; Fackler, J. P., Jr.; Porter, L. C. *Inorg. Chem.* **1989**, *28*, 2150–2154.

(7) Inoguchi, Y.; Milewski-Mahrla, B.; Schmidbaur, H. *Chem. Ber.* **1982**, *115*, 3085–3095.

(8) Mazany, A. M.; Fackler, J. P., Jr. *J. Am. Chem. Soc.* **1984**, *106*, 801–802.

(9) Grohmann, A.; Schmidbaur, H. In *Comprehensive Organometallic Chemistry II*; Wardell, J., Abel, E. W., Stone, F. G. A., Wilkinson, G., Eds.; Pergamon: Oxford, 1995; Vol. 3, pp 1, and references therein.

(10) Schmidbaur, H.; Grohmann, A.; Olmos, M. E. In *Gold, Progress in Chemistry, Biochemistry and Technology*; Schmidbaur, H., Ed.; John Wiley & Sons: Chichester, 1999; p 747, and references therein.

(11) Schmidbaur, H.; Wohlleben, A.; Wagner, F. E.; van de Vondel, D. F.; van der Kelen, G. P. *Chem. Ber.* **1977**, *110*, 2758–2764.

(12) Fackler, J. P., Jr. *Polyhedron* **1997**, *16*, 1–17.

(13) Calabro, D. C.; Harrison, B. A.; Palmer, G. T.; Moguel, M. K.; Rebert, R. L.; Burmeister, J. L. *Inorg. Chem.* **1981**, *20*, 4311–4316.

(14) Fackler, J. P., Jr.; Trzcinska-Bancroft, B. *Organometallics* **1985**, *4*, 1891–1893.

(15) Raptis, R. G.; Porter, L. C.; Emrich, R. J.; Murray, H. H.; Fackler, J. P., Jr. *Inorg. Chem.* **1990**, *29*, 4408–4412.

(16) Laguna, A.; Laguna, M. *Coord. Chem. Rev.* **1999**, *193–195*, 837–856.

(17) Laguna, M.; Cerrada, E. In *Metal Clusters in Chemistry*; Braunstein, P., Oro, L. A., Raithby, P. R., Eds.; Wiley-VCH: Weinheim, 1999; Vol. 1, p 459, and references therein.

(18) Schmidbaur, H.; Franke, R. *Inorg. Chim. Acta* **1975**, *13*, 79–83.

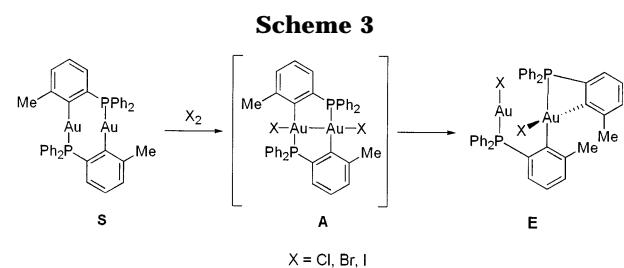
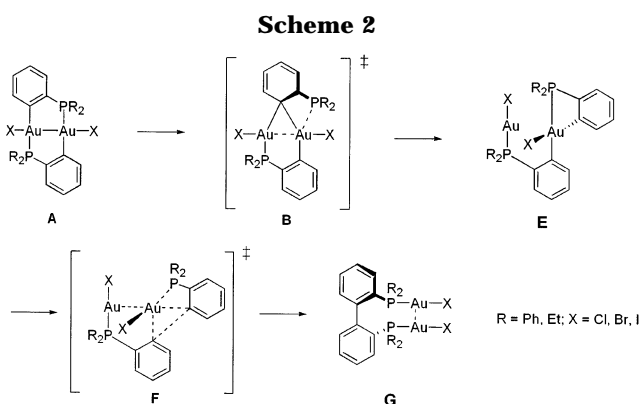
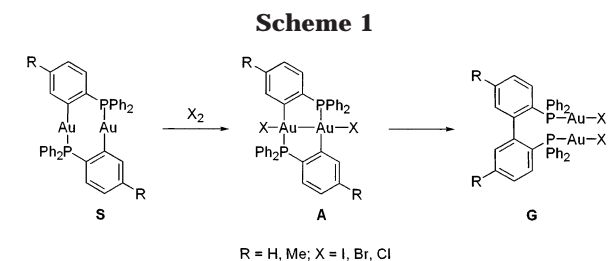
(19) Dudis, D. S.; Fackler, J. P., Jr. *Inorg. Chem.* **1985**, *24*, 3758–3762.

(20) Bennett, M. A.; Bhargava, S. K.; Griffiths, K. D.; Robertson, G. B.; Wickramasinghe, W. A.; Willis, A. C. *Angew. Chem., Int. Ed. Engl.* **1987**, *26*, 258–260.

(21) Bennett, M. A.; Bhargava, S. K.; Griffiths, K. D.; Robertson, G. B. *Angew. Chem., Int. Ed. Engl.* **1987**, *26*, 260–261.

(22) Bennett, M. A.; Bhargava, S. K.; Hockless, D. C. R.; Welling, L. L.; Willis, A. C. *J. Am. Chem. Soc.* **1996**, *118*, 10469–10478.

(23) Bhargava, S. K.; Mohr, F.; Bennett, M. A.; Welling, L. L.; Willis, A. C. *Organometallics* **2000**, *19*, 5628–5636.



2 shows the proposed reaction pathway for the isomerization of the digold(II) complexes (A), based on spectroscopic and kinetic evidence.<sup>22,24</sup>

The first step toward carbon–carbon coupling involves isomerization to a heterovalent gold(I)/gold(III) complex (E) via  $\sigma$ -aryl migration of the bridging ligand (B). In the second step, reductive elimination via (F) occurs at the gold(III) center to give the C–C coupled product (G).<sup>22,24</sup> Surprisingly, the reactivity changes if methyl substituents are present in the 6-positions (i.e., ortho to gold). In this case the initially formed digold(II) complexes rapidly isomerize to heterovalent gold(I)/gold(III) complexes and C–C coupling is not observed nor can it be induced (Scheme 3).<sup>23</sup>

To investigate possible reasons for this unusual ortho-effect, the course of this coupling reaction and the intermediates involved were investigated by applying quantum chemical ab-initio calculations on a series of model compounds. Furthermore we were interested in finding explanations for the different isomerization rates that have been observed for the digold(II) complexes containing Cl, Br, and I ligands.

## 2. Computational Details

All computations were carried out using the Gaussian98<sup>25</sup> software package running on a 16-processor Silicon Graphics Origin 2000. The Los-Alamos scalar relativistic pseudopotential for P, Cl, Br, I, and Au together with the corresponding

(24) Bennett, M. A.; Hockless, D. C. R.; Rae, A. D.; Welling, L. L.; Willis, A. C. *Organometallics* **2001**, *20*, 79–87.

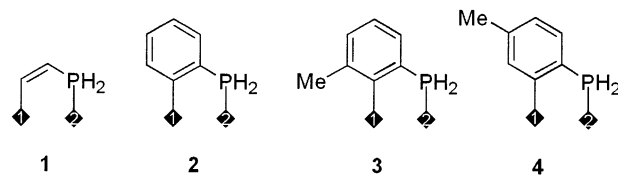


**Figure 1.** Schematic representation of the model ligands  $C_2H_2PH_2$  (1),  $C_6H_4PH_2$  (2), 6-Me $C_6H_3PH_2$  (3), and 5-Me $C_6H_3PH_2$  (4) as used in the calculations.

valence basis set (LANL2DZ)<sup>26</sup> as implemented in the software<sup>25</sup> were used in conjunction with second-order Møller–Plesset perturbation theory (MP2). For the lighter atoms we employed Dunning–Huzinaga valence- $\zeta$  basis sets.<sup>27</sup> To simplify the model and save computation time, the phenyl groups on the phosphorus atom were replaced by protons. All structures were fully optimized and for X = Cl proven to be either minima or first-order saddle points by analyzing the second-order derivative matrix (Hessian) at the MP2 level. For some of the larger molecules the location of the transition state was a nontrivial issue and turned out to be very demanding of computer time because the reaction paths involved large changes in a number of internal coordinates. Therefore, f-functions for gold were omitted, resulting in auriphilic interactions being underestimated. We point out, however, that this is probably compensated by the neglect of basis set superposition error corrections and the fact that MP2 often overestimates dispersive type of interactions.

## 3. Results and Discussion

Initially, the simple model ligand  $C_2H_2PH_2$  (1) (Figure 1) was used to calculate all possible intermediates and transition states involved in the reaction. We then extended our studies by using the larger aromatic model ligands  $C_6H_4PH_2$  (2), 6-Me $C_6H_3PH_2$  (3), and 5-Me $C_6H_3PH_2$  (4) to allow for a better comparison with the original ligands used in experimental by Bennett and co-workers.<sup>23</sup> The intermediates and transition state structures that have been calculated for the model ligand 6-Me $C_6H_3PH_2$  (3) are shown in Figure 2; the relative energy differences for the corresponding intermediates are listed in Table 1.

After the initial exothermic oxidative addition of  $X_2$  (X = Cl, Br, I) to the digold(I) starting material (S) isomerization of the digold(II) complex (A) to the gold(I)/gold(III) complex (E) via the transition state (B) occurs.<sup>28</sup> Further isomerization of E via the transition state (F) finally leads to the carbon–carbon coupled product (G). From the data shown in Table 1 it is obvious that for the simplest ligand ( $C_2H_2PH_2$ , 1) the minimum (1-E) and the transition states (1-B and 1-F)

(25) Frisch, M. J.; Trucks, G. W.; Schlegel, H. B.; Scuseria, G. E.; Robb, M. A.; Cheeseman, J. R.; Zakrzewski, V. G.; Montgomery, J. A., Jr.; Stratmann, R. E.; Burant, J. C.; Dapprich, S.; Millam, J. M.; Daniels, A. D.; Kudin, K. N.; Strain, M. C.; Farkas, O.; Tomasi, J.; Barone, V.; Cossi, M.; Cammi, R.; Mennucci, B.; Pomelli, C.; Adamo, C.; Morokuma, S.; Malick, D. K.; Rabuck, A. D.; Raghavachari, K.; Foresman, J. B.; Cioslowski, J.; Ortiz, J. V.; Baboul, A. G.; Stefanov, B. B.; Liu, G.; Fox, A.; Kieth, T.; Al-Laham, M. A.; Peng, C. Y.; Nanayakkara, A.; Gonzalez, C.; Gonzalez, A. C.; Head-Gordon, M.; Replogle, E. S.; Pople, J. A. *Gaussian 98*, revision A.7; Gaussian Inc.: Pittsburgh, PA, 1998.

(26) (a) Hay, P. J.; Wadt, W. R. *J. Chem. Phys.* **1985**, *82*, 270–289. (b) Wadt, W. R.; Hay, P. J. *J. Chem. Phys.* **1985**, *82*, 284–298. (c) Hay, P. J.; Wadt, W. R. *J. Chem. Phys.* **1985**, *82*, 299–310.

(27) Dunning, T. H.; Hay, P. J. In *Modern Theoretical Chemistry*; Scheafer, H. F., II, Ed.; Plenum: New York, 1976; pp 1–28.

(28) A further minimum (1-C) and a transition state (1-D) between 1-B and 1-E were found only for ligand 1 and not for the aromatic ligands 2, 3, and 4, and are therefore omitted from Figure 2 for clarity.

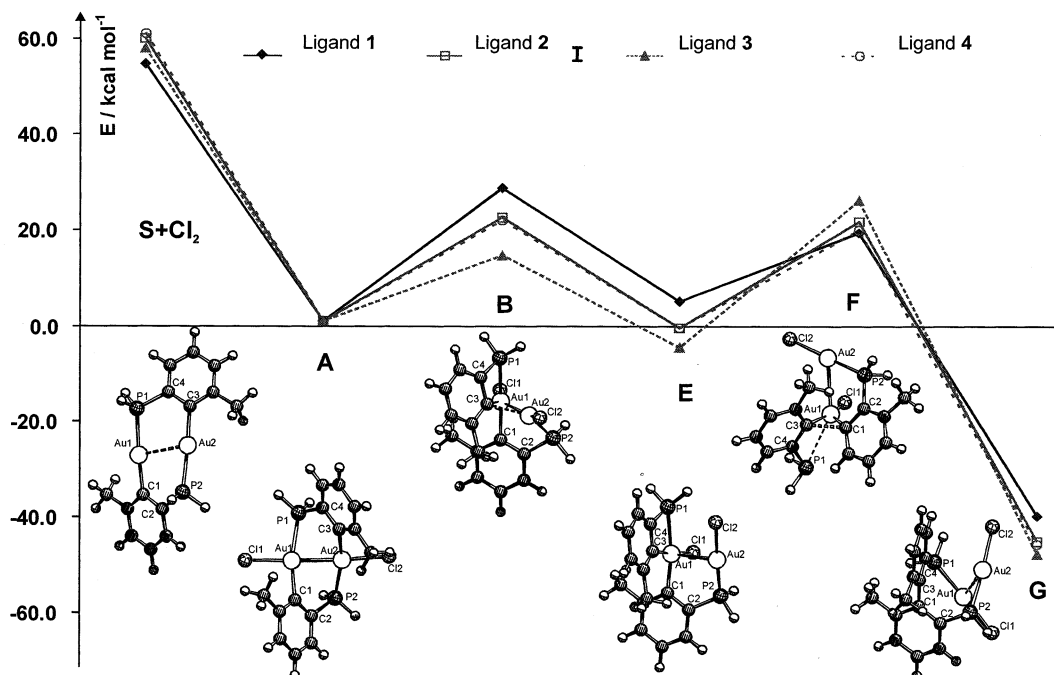


**Figure 2.** Suggested reaction course for the oxidative addition of chlorine to the digold(I) complex  $[\text{Au}_2(\mu\text{-L})_2]$  ( $\text{L}$  = ligands **1**, **2**, **3**, and **4**) (**S**). The energy profiles include the minima **A** and **E**, the transition states **B** and **F**, and the product **G**. The calculated structures are shown for ligand **3**.

**Table 1. Relative Energies [kcal mol<sup>-1</sup>] of the Different Compounds A–G, S + X<sub>2</sub>, and A' (The Reaction Course Is Shown in Figure 2)**

ligand	X	S + X <sub>2</sub>	A	B	E	F	G	A'
<b>1</b>	Cl	54.4	0.0	28.2	4.0	18.7	-41.5	0.0
	Br		0.0	26.7	6.2			0.0
	I		0.0	24.5	7.2	16.4	-40.5	0.0
<b>2</b>	Cl	59.8	0.0	21.8	-1.5	21.0	-47.0	4.9
	Br		0.0	20.2	0.4			6.3
	I		0.0	17.9	1.2		-46.3	8.8
<b>3</b>	Cl	57.5	0.0	13.9	-5.7	25.5	-49.7	25.7
	Br		0.0		-4.3			28.5
	I		0.0		-3.6		-49.0	33.3
<b>4</b>	Cl	61.0	0.0	21.2	-1.5	19.2	-47.4	5.1

are energetically less stable than the digold(II) complex **1-A**; only the C–C coupled product **1-G** is 41.5 kcal/mol more stable than **1-A**. According to the transition state energies, the rate-determining step seems to be the transformation of **1-A** via **1-B** (28.2 kcal/mol) to **1-E**.<sup>29</sup> Furthermore, for ligand **1** the gold(I)/gold(III) complex (**1-E**) is higher (4.0 kcal mol<sup>-1</sup>) in energy than the **E** structures of the aromatic ligands **2** (-1.5 kcal mol<sup>-1</sup>), **3** (-5.7 kcal mol<sup>-1</sup>), and **4** (-1.5 kcal mol<sup>-1</sup>) and in contrast to the aromatic ligands **1-E** is not easily accessible due to the high barrier (28.2 kcal mol<sup>-1</sup>) of the transition state (**1-B**) involved. This is partly due to the different starting geometries of the digold(II) species (**A**). While for **1-A** a  $C_s$  symmetric structure with a perfectly planar AuPCC–AuPCC eight-membered ring (dihedral angles  $\tau(\text{PAuAuP}) = 180^\circ$ ,  $\tau(\text{CAuAuC}) = 180^\circ$ ) is found, all other ligands **2**, **3**, and **4** show substantial bending of the AuPCC–AuPCC ring for **2-A**, **3-A**, and **4-A**. This is in good agreement with the X-ray crystal structure of  $[\text{Au}_2\text{I}_2(\mu\text{-C}_6\text{H}_4\text{PPh}_2)_2]$ , in which dihedral

angles of  $\tau(\text{PAuAuP}) = 139.7^\circ$  and  $\tau(\text{CAuAuC}) = 142.0^\circ$  were measured.<sup>21</sup> This bending seems to be slightly dependent on the substitution pattern on the aromatic ring, as it ranges from  $\tau(\text{PAuAuP}) = 144.3^\circ$  and  $\tau(\text{CAuAuC}) = 137.1^\circ$  for **2-A**, to  $\tau(\text{PAuAuP}) = 144.1^\circ$  and  $\tau(\text{CAuAuC}) = 136.8^\circ$  for **4-A**, to  $\tau(\text{PAuAuP}) = 136.1^\circ$  and  $\tau(\text{CAuAuC}) = 128.1^\circ$  for **3-A**.

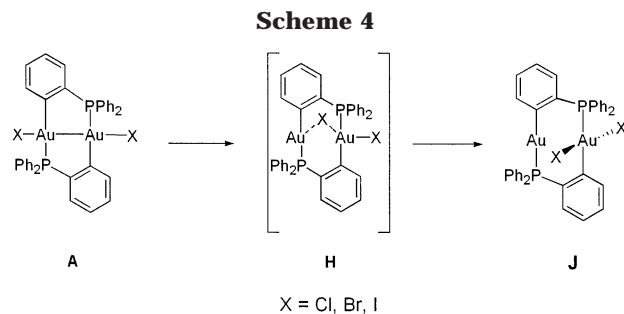
The stronger bending of the eight-membered ring in **3-A** compared to **2-A** and **4-A** compared to no bending in **1-A** clearly indicates that this is due to steric effects. In **2-A** and **4-A** there is enough space between the axial halide ligands and the ring protons, whereas the close proximity of the axial halide ligands and the 6-methyl groups in **3-A** leads to overcrowding and more pronounced bending. This is confirmed by energy differences between the planar (the structures calculated with fixed  $\tau(\text{CAuAuC}) = 180^\circ$  are denoted **A'**) and bent **A** structures, which are 4.9 kcal mol<sup>-1</sup> (**2-A'**), 25.7 kcal mol<sup>-1</sup> (**3-A'**), and 5.1 kcal mol<sup>-1</sup> (**4-A'**). Furthermore we observed further bending of the Au–Au–X angle in the flat,  $C_s$  symmetric **A'** structures with an Au–Au–Cl angle of 152.8° compared to 171.2° ( $\Delta\alpha = 18.4^\circ$ ) for the bent ring in **3-A**. For **2-A'** and **4-A'** somewhat smaller differences ( $\Delta\alpha = 9.4^\circ$  and  $\Delta\alpha = 9.6^\circ$ , respectively) were found. Further evidence arises from a comparison of the shortest nearest neighbor C···H contacts in the planar structures, which range from 285.3 pm (**1-A'**) to 247.3 pm/246.5 pm (**2-A'**)/(**4-A'**) and 202.7 pm for **3-A'**, while for the bent structures much longer and only slightly different distances of 285.3 pm (**1-A**), 279.6 pm (**2-A**), 279.1 pm (**4-A**), and 284.2 pm (**3-A**) were calculated. In comparison, the I···H (ring proton) distance in  $[\text{Au}_2\text{I}_2(\mu\text{-C}_6\text{H}_4\text{PPh}_2)_2]$  was measured to be 295.5 pm.<sup>21</sup>

The bending of the eight-membered ring seems to affect the accessibility of the transition state **B**, in that a stronger bending in **A** results in a lower activation

(29) With energies of 12.6 and 13.5 kcal mol<sup>-1</sup> above **1-A** the structures **1-C** and **1-D** do not affect the transformation via **1-B** to **1-E**.

energy to transition state **B**. The Au1–C3 distances in **A** decrease to 350.6 pm (**1-B**), 335.8 pm (**2-B**), 335.1 pm (**4-B**), and 324.7 pm (**3-B**) in accordance with decreasing energy barriers for transition state **B** (Table 1). It is evident that the stronger bending of the eight-membered AuPCC–AuPCC ring in **3-A** caused by the methyl substituent in the ortho position to gold lowers the barrier to **B** for the isomerization of **A** to **E** by more than 14 kcal mol<sup>-1</sup> compared to **1-A**.

It is interesting to note that the gold(I)/gold(III) species (**2-E** and **4-E**) are only slightly more stable (by 1.5 kcal mol<sup>-1</sup>) than the digold(II) complexes (**2-A** and **4-A**). In contrast, the 6-methyl-substituted gold(I)/gold(II) complex (**3-E**) is considerably more stable (by 5.7 kcal mol<sup>-1</sup>) than the digold(II) isomer (**3-A**). Closer examination of the next reaction step (gold(I)/gold(III) **E** to the C–C coupled products **G**) reveals that the varying stability of **E** and also the transition state barrier for **F** are responsible for the different reaction products observed. Starting from **1-E** there is a moderate energy barrier of 14.7 kcal mol<sup>-1</sup> to the transition state **1-F**, which leads easily to C–C bond formation and finally to the very stable product **1-G** (–41.5 kcal mol<sup>-1</sup> compared to **A**). For the compounds containing ligands **2** and **4** this barrier is considerably higher (22.5 and 20.7 kcal mol<sup>-1</sup> for **2-F** and **4-F**, respectively). For the 6-methyl-substituted ligand (**3**) this energy barrier amounts to more than 30 kcal mol<sup>-1</sup>! The reason for this dramatic increase (31.2 kcal mol<sup>-1</sup> for **3-F** compared to **3-E**) originates from the high stability of **3-E** compared to all other gold(I)/gold(III) complexes and, even more importantly, from the higher steric demand of the methyl group at the C3 atom in the transition state **3-F**. The search for transition states of **F** was very complicated and computer time demanding because this particular reaction path involves large changes in a number of internal coordinates. In the transition states (**F**, X = Cl), the Au1–P1 bonds are almost cleaved, i.e., Au1–P1 = 352.3 pm (**1-F**), 325.0 pm (**2-F**), 309.5 pm (**3-F**), and 327.1 pm (**4-F**). In addition, both carbon–gold bonds (Au1–C1 and Au1–C3) are elongated [Au1–C1 = 209.0 pm/Au1–C3 = 210.2 pm (**1-F**), 213.8 pm/215.1 pm (**2-F**), 216.2 pm/216.3 pm (**3-F**), and 213.4 pm/214.4 pm (**4-F**)] and obviously share the same  $\sigma$ -type orbital of the gold atom. These results are in contrast to the original hypothesis,<sup>22</sup> as it is not reversible loss of an axial halide ligand that initiates C–C bond formation, but rather partial opening of the Au<sup>III</sup>–P bond that allows this reaction step to occur. Moreover the Au–Cl bonds help to stabilize the transition states **F** as the Au–Cl bonds shrink in all cases to distances (238.2 to 240.0 pm) below the values found in the products **G** (240.6 to 240.8 pm). The arrangement of the transition state **F** explains why C–C bond formation is not observed for the 6-methyl-substituted ligand. The steric effect of the methyl group at C3 makes bond formation especially difficult, which is documented in the much longer Au–C1 and Au–C3 bond distances (216.2 and 216.3 pm), a shorter Au1–P1 bond, and a much shorter Au–Au bond distance (299.3 pm) compared to the other **F** complexes. These structural changes in **3-F** are obviously necessary to compensate



for the steric effect and to stabilize the transition state but eventually leads to a much higher transition state energy.

It has also been suggested that another isomeric gold(I)/gold(III) complex (**J**) and a corresponding transition state **H** might be intermediates in the C–C coupling process (Scheme 4).<sup>22</sup> However, our calculations indicate that this cannot be the case: for X = Cl and ligand **1** (ligand **2**) the transition state barrier of **H** (compared to **A**) is found to be 31.9 kcal mol<sup>-1</sup> (31.4 kcal mol<sup>-1</sup>) and, at least in the case of ligand **2**, substantially higher than the transition states **B** (21.8 kcal mol<sup>-1</sup>) and **F** (21.0 kcal mol<sup>-1</sup>) (Table 1). Nevertheless it is interesting that the calculated **J** isomers are again quite similar in energy for the different ligands.

The experimentally observed reaction rates for the digold(II) (**A**) to gold(I) biphenyl (**G**) isomerization are in the order I > Br ≫ Cl.<sup>22</sup> According to our calculations, this cannot be explained by a higher stability of the bromo or iodo gold(I)/gold(II) complexes and the gold(I) biphenyl compounds (**G**). The observed order of isomerization rates is due to the energetically lower transition states **B** and **F** for the heavier halides. Relative to the corresponding **A** compounds the complexes **1-E** (6.2 kcal mol<sup>-1</sup>), **2-E** (0.4 kcal mol<sup>-1</sup>), and **3-E** (–4.3 kcal mol<sup>-1</sup>) (X = Br) are calculated to be less stable compared to X = Cl (4.0, –1.5, and –5.7 kcal mol<sup>-1</sup>); see Table 1. Even more unstable, in comparison to X = Cl, are the iodo gold(I)/gold(III) compounds (**E**), with values of 7.2 (**1-E**), 1.2 (**2-E**), and –3.6 (**3-E**) kcal mol<sup>-1</sup>. The same is true in the case of iodine (X = I) for the gold(I) biphenyl products **1-G**, **2-G**, and **3-G** (–40.5, –46.3, and –49.0 kcal mol<sup>-1</sup>), which are higher in energy as well (Table 1). However, this trend reverses for the transition state energies of **B** and **F** (at least for the calculated structures **1-B**, **2-B**, and **1-F**), which are lower in energy for the heavier halides compared to the chloro derivatives. For X = I (compared to X = Cl) we obtain values of 24.5 (28.2) kcal mol<sup>-1</sup> (**1-B**), 16.4 (18.7) kcal mol<sup>-1</sup> (**1-F**), and 17.9 (21.8) kcal mol<sup>-1</sup> (**2-B**).

As the bromo and iodo complexes show only small structural differences in their geometries, it is quite unexpected that the transition states **B** and **F** are lower in energy while the **A**, **E**, and **G** complexes are higher. From a structural point of view this is difficult to rationalize, but one reason could be a more pronounced aurophilic interaction stabilizing the transition states **B** and **F** for the bromo and especially for the iodo compounds. The Au–Au bond distances are (independent from the ligands) shorter in the chlorine **A** and **E** species than in the corresponding bromo and iodo complexes (Table 2); that is, for **2-A** (**2-E**) we find Au–Au distances of 264.0 pm (311.2 pm), 265.9 pm (313.4 pm), and 268.0

**Table 2. Gold–Gold Bond Distances [pm] for All Calculated Compounds A–G and A'**

ligand	X	A	B	E	F	G	A'
<b>1</b>	Cl	268.0	276.7	312.7	316.6	331.2	268.0
	Br	270.7	277.3	314.9			270.7
	I	274.1	277.9	316.3	315.3	321.5	274.1
<b>2</b>	Cl	264.0	272.6	311.2	312.6	317.7	270.7
	Br	265.9	273.0	313.4			271.3
	I	268.0	273.3	315.9		314.4	279.7
<b>3</b>	Cl	261.2	273.0	311.2	299.3	318.9	283.9
	Br	263.1		309.4			290.9
	I	265.1		310.6		315.3	300.4
<b>4</b>	Cl	263.9	272.5	311.3	317.6	318.9	270.6

pm (315.9 pm) for X = Cl, Br, and I. However, in the transition states **B** the Au–Au bond distances are almost equal, i.e., 272.6, 273.0, and 273.3 pm for X = Cl, Br, and I in **2-B**. Even more surprising is the transition state **1-F**. In the case of X = Cl a rather long Au–Au distance of 316.6 pm is calculated compared to the corresponding iodo compound. Moreover, in the case of X = I the Au–Au distance gets shorter going from **1-E** to **1-F**, in contrast to the chlorine compound. A similar effect (shorter Au–Au bond distances) is also found in the sterically very demanding transition state **3-F**, which suggests that aurophilic interactions help to compensate for an energetically unfavorable situation. These results are consistent with other theoretical work, which has shown that the Au...Au attraction in compounds of the type [X<sub>2</sub>AuPH<sub>3</sub>]<sub>2</sub> is much stronger for iodo and bromo than it is for chlorine.<sup>30</sup> A further reason might be the more pronounced bending of the eight-membered AuPCC–AuPCC ring in the bromo and iodo **A** compounds. It is possible that, at least for the first reaction step (**A** to **E**), the same argument that holds for the different ligands (**1–4**) is also true for the different halides: stronger bending of the AuPCC–AuPCC ring allows for an easier access via **B** to the gold(I)/gold(III) structures **E**.

Finally, it is interesting to note that for other axial ligands such as benzoate, acetate, or nitrate no isomerization to either gold(I)/gold(III) (**E**) or gold(I) biphenyl

complexes (**G**) has been observed; the reaction stops at the digold(II) product (**A**).<sup>22,24</sup> According to our calculations, this is consistent with the higher steric demand since, for example, a benzoate ligand is much bulkier than a halide, making it difficult to reach a **B** type transition state. Furthermore, the experimentally determined X-ray structure of the bis(benzoato)digold(II) complex containing the C<sub>6</sub>H<sub>4</sub>PET<sub>2</sub> ligand has a very short and presumably strong Au–Au bond (252.4 pm),<sup>22</sup> which may raise the transition state barrier to the gold(I)/gold(III) product (**E**) as well.

#### 4. Conclusions

By using quantum chemical calculations we have been able to determine intermediates and transition states involved in the well-studied isomerization reaction of binuclear cycloaurated digold(II) complexes of the type [Au<sub>2</sub>X<sub>2</sub>(μ-L)<sub>2</sub>] (X = Cl, Br, I and L = C<sub>6</sub>H<sub>4</sub>PR<sub>2</sub>, 5-MeC<sub>6</sub>H<sub>3</sub>PR<sub>2</sub>, 6-MeC<sub>6</sub>H<sub>3</sub>PR<sub>2</sub>). The reaction course is in agreement with the experimentally known intermediates. The marked difference in reactivity between the 6-methyl ligand (6-MeC<sub>6</sub>H<sub>3</sub>PR<sub>2</sub>) and the ligand C<sub>6</sub>H<sub>4</sub>PR<sub>2</sub> (or the 5-methyl ligand 5-MeC<sub>6</sub>H<sub>3</sub>PR<sub>2</sub>) is mainly due to an unusually strong ortho effect of the 6-methyl group. In the first part of the reaction the 6-methyl group is responsible for a stronger bending of the eight-membered AuCCP–AuCCP ring. This bending lowers the transition state barrier in the first reaction step (**3-B**) and favors isomerization to the gold(I)/gold(III) complexes **3-E**. In the second step of the reaction, the 6-methyl group has an opposite effect by causing a strong steric hindrance in the transition state **3-F**, which makes C–C bond formation and hence the carbon–carbon coupled product (**3-G**) inaccessible, which is in good agreement with experimental findings.<sup>23</sup>

**Acknowledgment.** The authors wish to thank the Alexander von Humboldt Foundation (Bonn, Germany), the Marsden Fund (Wellington, New Zealand), and the Auckland University Research Committee for support for this work. F.M. thanks the Australian Government for the award of an APA Scholarship.

(30) Pyykkö, P.; Li, J.; Runeberg, N. *Chem. Phys. Lett.* **1994**, *218*, 133–138.